We are IntechOpen,
the world's leading publisher of
Open Access books
Built by scientists, for scientists

4,800
Open access books available

122,000
International authors and editors

135M
Downloads

Our authors are among the

154
Countries delivered to

TOP 1%
most cited scientists

12.2%
Contributors from top 500 universities

CLARIVATE ANALYTICS

BOOK CITATION INDEX

INDEXED

WEB OF SCIENCE™

Selection of our books indexed in the Book Citation Index
in Web of Science™ Core Collection (BKCI)

Interested in publishing with us?
Contact book.department@intechopen.com

Numbers displayed above are based on latest data collected.
For more information visit www.intechopen.com

Green Water Treatment for Pharmaceutical Pollution

Nilce Ortiz

Abstract

Environmental sustainability demands the advancement in water treatment and the use of lighting natural resources. Brazil has one of the most stable and intense solar irradiation in the world. It has to be used not only for energy generation purposes but also and mostly for water treatment, water quality polishment, and furthermore water disinfection. The chapter performs a comparison of different green technologies for water treatment as natural solar irradiation, simulated solar photolysis, solar photo-Fenton with and without hydrogen peroxide addition (solar/Fe), solar photo-Fenton with and without peroxide (solar/Fe/H_2O_2), titanium oxide-mediated photocatalysis (UV/TiO_2), photolysis under UV irradiation, and UV treatment with hydrogen peroxide (UV/H_2O_2). The chapter describes the solar photodecomposition calculations for pharmaceuticals and the emerging pollutants mostly found in polluted waters, including the decomposition route, kinetics, and process parameters. Many published works to point out the important properties to evaluate catalyzer and semiconductor materials after their use in photodecomposition processes. The essay includes the solar photodecomposition of dyes, carbamazepine, hormones, acetaminophen, antipyrine, bisphenol A, antibiotics, and the photodecomposition by-products. Finally, the chapter presents the synergistic effect between them with the probable mechanism and mineralization degree.

Keywords: pharmaceuticals, antibiotics, TiO_2, semiconductor, solar, photodecomposition

1. Introduction

The environmental performances are estimated using the life cycle assessment and the effective removal of 1 µg of 17α-ethynylestradiol (ES) for 1 liter of wastewater. The choice of ES was due to being a worldwide common micropollutant and endocrine-disrupting chemicals (EDCs) in a functional unit [1]. The natural solar photolysis exhibited an environmental footprint about 23 times greater than solar/Fe systems. The solar/Fe/H_2O_2 minimized the environmental footprint with the energy-intensive simulated solar irradiation that had a much higher, about five times, environmental footprint than the natural solar light. The UV photolysis also shows a low environmental impact. The TiO_2 addition to UV and H_2O_2 to UV reduced the environmental impact of about 97% and 88%, not considering the footprint of the TiO_2 production [2].

The total environmental footprint and the environmental sustainability of all the photodecomposition processes were directly proportional to water treatment efficiency and inversely proportional to treatment time (substantial energy input

per time unit). The addition of TiO_2, iron, and H_2O_2 improved the process efficiency and environmental sustainability considering only the electricity consumption; the introduction of renewable energy resources could reduce the environmental footprint of the oxidation processes by up to 87.5%.

A solar spectrum contains approximately 46% of infrared light, 4% of UV light, and 50% of visible light. Such natural radiation composition highlight the importance of the visible-light-responsive TiO_2 development for natural and renewable solar photodecomposition applications. TiO_2 displays photocatalytic role when irradiated by ultraviolet (UV) due to its large bandgap (3.0 eV for rutile and 3.2 eV for anatase). The development of visible light-responsive TiO_2 includes chemical doping and photosensitization. The chemical doping is used to narrow the bandgap of TiO_2; the doped ions in TiO_2 act as recombination centers for photoexcited electrons and holes decreasing the photocatalytic activity.

The organic dye photosensitization on TiO_2 represents the major limitation for applications due to the poor dye stability, which can undergo desorption, photolysis and oxidative degradation, and fastback electron transfer, which results in low quantum yield for the photocatalytic reaction. An alternative for organic dye use in the metallic nanoparticles (NPs) is used successfully as photosensitizers for TiO_2 due to their stability and strong photoabsorption under visible light based on surface plasmon resonance [3]. It is a coherent oscillation of electrons on the metallic NP surfaces during the incident light irradiation.

The TiO_2 photosensitizers were first described in 2005 using gold (Au) as nanoparticles with TiO_2 (Au/TiO_2) the resultant film oxidized the ethanol and methanol at the expense of oxygen reduction under visible light radiation. The use of Au/TiO_2 for 2-propanol decomposition is induced by surface plasmon resonance photocatalytic process: (1) the Au NP adsorption of photons, (2) the Au NP electrons are injected into the conduction band of TiO_2, and (3) the resultant electron-deficient Au NPs can oxidize 2-propanol to recover to the fundamental metallic Au NP state. The pharmaceutical waste in the environment cause adverse health effects in the reproductive, neurological, and immune systems of wildlife and humans. Commonly they are resultant of agricultural lands' runoff, septic tanks' leakage, and the discharge of sewage treatment plants' effluents [4]. They can cause significant severe environmental damage even in trace concentrations. Worldwide EDCs are continuously released, and the efficiency of conventional water treatment technologies against such contaminants is minimal.

Advanced oxidation processes (AOPs) are a promising technology for the removal of the persistent organic pollutants (POPs), such as pharmaceuticals and endocrine disrupters (EDCs) from polluted waters. The photocatalytic methods are likely the most promising, especially those involving visible light-responsive materials, i.e., heterogeneous solar photocatalysis.

The photocatalytic hydroxide radicals are potent oxidants and react fast and unselectively with surrounding chemical species via radical addition, hydrogen abstraction, or e- transfer mechanisms. Many oxidant species can also degrade the pharmaceuticals and endocrine disrupter compounds in some cases the intermediate compounds present higher decomposition effectiveness and ends up in complete mineralization with the production of CO_2, H_2O, and inorganic salts.

The mass transfer is the controlled slowest step of the photodecomposition reaction of adsorption/desorption. The reaction requires the reactant adsorption/desorption on the catalyst surface and the presence of any barrier to reduce the reaction efficiency. Some experiments are performed keeping the reactor under dark conditions until the adsorption process reaches the equilibrium with the adsorbed mass at the semiconductor surface. After that, the reactor is irradiated and produces the radicals acting in the adsorbent surface and also in the solution. The radiation and the semiconductor generate e^- and h^+ pairs and radicals.

2. Photodecomposition: kinetics and process parameters

The heterogeneous photocatalysis shows a strong dependence on the operating temperature. The kinetics is usually dependent on the first step of the adsorption and the equilibrium modeled by Langmuir isotherms and Langmuir-Hinshelwood model. The first pseudo-order usually appears at the beginning of the reaction, just in the initial steps. As the reaction proceeds, the intermediate production could interfere with the radiation incidence. The observed decomposition rates as the pollutant start to decompose and begin the competition for the adsorption sites between the pollutants and the adsorbed species. The initial pollutant concentration starts to be the limiting reactant with mass transfer limitations with no kinetic control for lower concentrations.

The increase of the catalyst mass promotes the photodegradation rate and the active catalyst sites. If the system is a slurry, the reaction rate reaches a maximum or optimal value and after that declines. The higher suspended particle concentration enhances the light scattering, the particle agglomeration, with light opacity enhancement, and after a certain point, the photodecomposition efficiency decreases. There is an equilibrium between the available surface site and the suspended particles control.

The oxygen plays a vital role in the photodecomposition reactions; dissolved O_2 reacts with the photogenerated electrons leading to O_2^- radicals and preventing the recombination of the generated e^- and the h^+ pairs. The comparison between the kinetics of the air-saturated solutions and the pure oxygen solution often results in smaller rates for the first.

The pH values influence the catalyst aggregations and its surface charges, with the valence band (VB) and conduction band (CB) position. At low pH values, the CB holes are more effective in comparison with VB. The change in the pH values allows the surface charge modification mostly when the amphoteric groups are present [5].

The adsorption equilibrium after decomposition depends on the pollutant pH speciation and the reactive species. Considering the low pH values, the h^+ can be the more oxidizing species, the amount of ˙OH increases under alkaline conditions when the OH^- ions are available to react with h^+, and the ˙OH become the primary oxidant (Eqs. (1) and (2)). This effect increases the ˙OH availability at higher pH values in spite of the negatively charged catalyst surface and also the pollutant repelling action at such pH values; the ˙OH radicals' attack can explain the pH medium behavior.

$$(M - OH)surface + H^+ < = > (M - OH_2^+)surface \qquad (1)$$

$$(M - OH)surface + OH^- < = > (M - O^-) surface + H_2O \qquad (2)$$

The presence of some anions like chloride, nitrate, and sulfate reduces the photocatalytic performance as a result of the competition for the adsorption sites to scavenge the ˙OH radicals. Natural organic matter and humic acids are scavengers of the reactive species and usually show negative photodegradation influence. Nevertheless, the presence of the carbonate and bicarbonate increases photodecomposition efficiency.

The temperature has a limited effect in the photodecomposition efficiency until 80 C°; after that there is the tendency to reduce the photocatalytic efficiency as a result of lower oxygen solubility in water. Different temperatures can also promote intermediaries and by-product formation.

3. Semiconductor materials

Semiconductor photocatalytic process has shown great potential as a low cost, environment-friendly treatment technology in degrading a wide range of pollutants. The photocatalysis has the dependency of the reactive oxygen species formation by the semiconductor particle with light energy greater than the bandgap energy [4]. The TiO_2 photocatalyst has an important drawback of photocatalysis and with gap energy which is the use of UV light, corresponding with 3–5% of natural solar light.

Some modification on TiO_2 surface is one promising route to enable TiO_2 sensitive to visible light for water purification. A variety of strategies improve the photocatalytic efficiency from dispersed solids to second-generation photocatalysts (chemically doped and physically modified by dispersed solids) achieving better spectral sensitivity and photoactivity.

Published results indicate better results with inert materials as zeolite (TiO_2-FeZ) or TiO_2 (SnS_2). Zeolite showed high surface area but lower bandgaps in comparison with TiO_2 powder and decreases the efficiency following the FeZ and SnS_2 content [5]. The H_2O_2 addition enhanced solar-driven degradation and solar/TiO_2-FeZ with higher decomposition rates followed by solar/TiO_2-SnS_2 with 51%, TiO_2 P25 with 41.3%, and finally 34.4% for TiO_2-SnS_2/H_2O_2. The pseudo-first-order kinetics was the driving for solar photodecomposition with the higher rates for solar/TiO_2-FeZ/H_2O_2 with $K_1 = 15.39 \times 10^{-3}$ min^{-1} with more than twice of the solar/TiO_2-SnS_2 rate and three times more than solar/TiO_2, solar/TiO_2/H_2O_2, and solar/TiO_2-SnS_2/H_2O_2.

A challenge to be overcome is the presence of suspended solid particles in the reaction environment; they reduce the solar irradiance and the photocatalysis efficiency. The solid deposition over an inert material with the high surface area can fix and stabilize the solid particles. The engineering materials with transitional metals in surface deposition are a solution, like carbon nanotubes, dye sensitizers, conductive polymers, graphene oxide, and other semiconducting materials. The semiconductor supporting material has to avoid the agglomeration formation.

The commercial TiO_2 (P25) is the most common catalyzer in spite of lower azo decomposition; Ag_2O is another active photocatalyst with promising results for azo photodecomposition. Nevertheless, the use of Ag_2O in azo mixture showed faster degradation with better decomposition results due to the synergetic oxidation effect.

The scavengers' presence reduces the photodecomposition effect in water suspension. The ions HCO_3^-/CO_3^{2-}, SO_4^{2-}, Cl^-, and NO_3^- showed inhibitory effects toward the hydroxyl radicals generated by AOPs.

The natural organic matter (NOM) presence showed a synergistic effect increasing the E2 degradation, such degradation produces other radicals. Published studies relate to the degradation of the NOM species of humic acid and fulvic acid applied in solar/photodegradation resulting in all organic compounds that were mineralized after 150 min of treatment. The formed E2 intermediaries during the treatment do not possess any estrogen effect.

The addition of noble metals as Au and Ag increases the visible light ability with the manipulation of the optical properties and microstructure combined with inorganic and biotemplates as nanostructures of micelles, as spent tea leaf, trimethylammonium bromide, and metal nanoparticles improve the photodegradation efficiency. The use of Co_3O_4 spinel nanoparticles, NiO nano-sticks, the binary metal oxide nanocomposites of CeO_2/Y_2O_3 and NiO/MnO is effective in dye degradation of RhB, MB, MO, and rose bengal dye.

BiOCl has superior efficiency as photocatalysts due to the interlayer-specific structure of $[Bi_2O_2]_2^+$ with double Cl^- ions where the photogenerated e^- and h^+ pairs are separated. The BiOCl microspheres synthesized via ethylene glycol are mediated

by a solvothermal method with the visible light drive. The crystallinity, surface area, and optical and electronic properties of BiOCl samples depend on the reactant concentration with the benefit from the exposed (110) face and oxygen vacancy; BiOCl allows a maximum CBZ degradation efficiency of 70% after 180 min under visible light illumination. The kinetic rate constant (k) of CBZ degradation in synthetic BiOCl (0.0935 min^{-1}) was 52 times higher than the ordinary BiOCl (0.0018 min^{-1}). The improved photocatalytic activities for BiOCl were attributed to the combination of enhanced carbamazepine adsorption, increased with visible light drive and efficient separation of photogenerated e$^-$ and h$^+$ pairs. The trapping experiments of radicals and holes showed the $\cdot O_2^-$ and h$^+$ as dominant active species in the process and the most important; the BiOCl performance was also efficient in natural water without any additive. The experimental findings indicate the BiOCl photocatalysis is an efficient and cost-effective technology for recalcitrant pharmaceutical contaminant removal.

4. Dye photodecomposition

The higher development of the textile industry caused the emission of large quantities of dye wastewater with high chemical stability in surface water resources all over the world; the effect is the severe environmental damage and problems worldwide.

The advanced oxidation process (AOP) is in situ treatment technology and is widely applied on persistent, toxic, and poorly biodegradable organic pollutants.

The improvement of photodecomposition process reduces the by-products' and final products' toxicity. The biological methods are insufficient to decompose such stable organic compounds and chemical molecules. Industrial wastewater is a mixture of various components with high complexity and diversity. The interactions among the different components can occur, weakening and even blocking the photodecomposition effect. The heterogeneous photocatalysis is taking considerable attention to the textile wastewater treatment due to its low cost and low secondary by-product pollution. The disadvantages are the low quantum efficiency and slow reactant rate using the most common semiconductor, the TiO$_2$. The use of Ag$_2$O with a very narrow bandgap of 1.3 eV allows applying a wide range of the solar spectrum with an increase in the photodecomposition rate. The literature describes a photodecomposition process with last about 120 s to degrade the Methyl orange under UV and Visible light and 40 min with only Infrared light.

The application of the visible light photodecomposition in a dye mixture of methylene blue (MB), methyl orange (MO), and rhodamine (RH) indicates the MO as the more stable azo compound than the other organic pollutants due to the aromatic groups attached at the end of the azo bond. Despite this fact when the light-driven photodecomposition uses Ag$_2$O as a catalyzer, it was the fastest and easiest decomposed compound. Published results indicate the visible light photodecomposition with Ag$_2$O with the elimination of 90.2% of MO, 96.5% of RH, and 99.5% of MB using 4, 50, and 20 min, respectively.

In dye photodecomposition in acidic conditions, some peaks with higher absorbances change some wavelength numbers indicating the chemical structure transformation from hydrazone to azo form. Despite such change, the concentration still reduces with time, and the complete degradation of the dye mixture finished in 18 min at pH 3 and 15 min at pH 5. The observation of 90% of the total mineralization was after 50 min under acidic conditions and 40 min under neutral and alkaline conditions.

The dye mixture showed better decomposition results than only a single one; a synergistic oxidation phenomenon occurring in the photodegradation of the dye

mixtures with Ag_2O indicates no apparent photoreduction of Ag_2O, and the solid material still consisted of pure Ag_2O and can be used consequently as a high-performance catalyst for dye wastewater treatment.

5. Solar treatment for carbamazepine

The carbamazepine (CBZ) is widely used as antiepileptic and mood stabilizer, worldwide, and the consumption is about 1014 ton year^{-1}. The CBZ shows high stability and low biodegradability, and the removal percentage for conventional water treatment process is less than 10%. Almost all consumed CBZ is discharged as sewage in the water environment causing adverse effects on the surface water quality, ecosystem, and human health [6].

The CBZ photodegradation process catalyzed by TiO_2 and ZnO nanoparticles generates three derivatives: carbamazepine epoxide, acridine, and acridone. TiO2 is effective in degrading CBZ and carbamazepine epoxide. Considering the acridine and acridone, no significant differences were found between those two catalysts. The CBZ and carbamazepine epoxide photodegradation was affected by pH (especially in the presence of TiO_2 as NPs) and natural organic matter [7]. In contrast, the acridine and acridone photodegradation was not affected by pH and organic matter. The TiO_2 and ZnO catalysts present contrasted efficiency on CBZ decomposition when compared with its derivatives and the effect of environmental parameters on the CBZ as photodegradation efficiency of the derivatives' presence cannot be predicted based only on the parent molecule (CBZ) behavior. The indication of higher degradation efficiency was for higher initial concentrations with a degradation rate of 52 times greater than for lower initial concentrations, and the kinetics corresponds to pseudo-second-order.

The negatively charged CBZ is due to the presence of the amide bond, and the exposed surface of the semiconductor positively charged enhances the surface adsorption processes. The proton adsorption also improves the effectiveness of the catalyzed reaction under visible light radiation, promoting long-term stability and the catalyst reusability. The visible-light-driven photocatalytic activity enhancements are the synergetic effects, including a large absorption capacity, the promotion of the light harvestability, and high separation efficiency of photogenerated e$^-$ and h$^+$ pairs.

The use of some scavengers as $AgNO_3^-$ for e$^-$, HCOONa for h$^+$, and butanol for $\cdot$OH (radical) and the N_2 purging to detect the function of O2 elucidate the main active species involved in the photodegradation process. The addition of $NaHCO_2$ reduces the decomposition in 18% as an indication of the importance of the h$^+$ radical in the reaction. The addition of n-butanol or N_2 purging showed no different reaction efficiency; this effect implied the addition of O_2 produces the $\cdot O_2$ radicals and increases the CBZ degradation confirming the domination of the degradation process by oxidation step with the $\cdot O_2^-$ radical generation and partly by the direct h$^+$ oxidation process.

The CBZ (A) oxidation reaction results in four intermediaries B, C, and D. The compounds B, C, and D are intermediaries with high decomposition rate (**Figure 1**). The attack of the CBZ oleofinic bond in a central heterocyclic ring forms compound B. The generation of radicals and the oleofinic bond of CBZ decomposed in C and D. The compound C uses a ring contraction reaction followed by an intramolecular cyclization mechanism resulting in intermediate compound F. Finally the formation of compound G was by intramolecular cyclization mechanism of compound D.

The primary concern about the pharmaceutical photodecomposition is the possible formation of the toxic intermediate and by-products. The literature cited as possible toxic intermediates for CBZ photodecomposition, the CBZ-10, 11-epoxide,
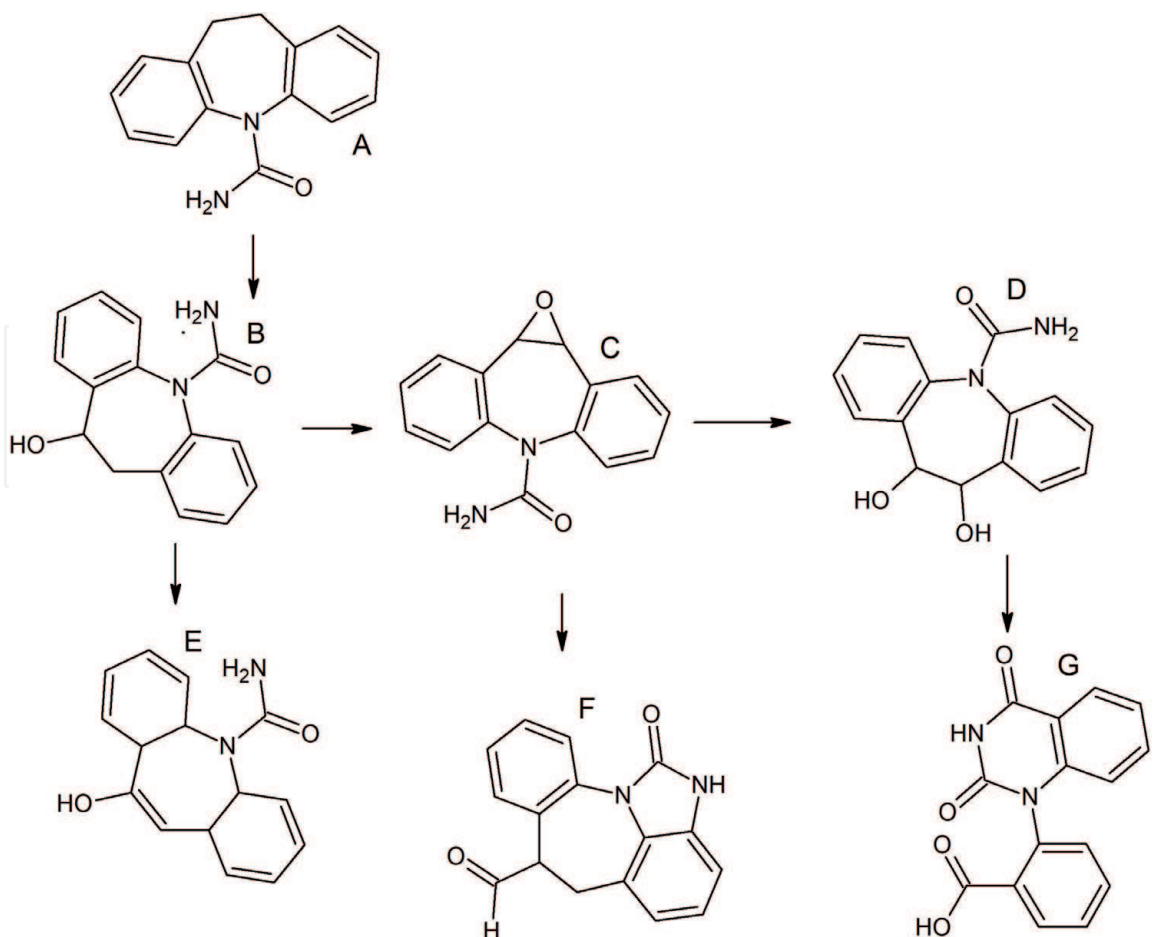
Figure 1.
The Carbamazepine degradation by-products.

and acridine. The photodecomposition optimization indicates BiOCl removed about 2–3 mg L^{-1} of CBZ after 150 min of solar irradiation, more than 78% of no toxic intermediaries. Always there will be the possibility to keep the photodecomposition reaction for a longer time of solar radiation. The recommendation is the use of adsorbent material, and after the absorption, removing the pharmaceuticals from the reaction media, and the photodecomposition reaction can keep continuing until mineralization and proper discharge.

6. Solar photodecomposition of hormones

The 17β-estradiol (E2) is the most natural estrogenic hormone occurring in sewage-polluted waters and also an intermediate key in the industrial synthesis of other estrogens. It is frequent in natural water environment with the high potential to hormonal disruption pathways in wildlife even in low nanogram concentrations. Recently, it was added to the watch list of priority substances in the EU Water Framework Directive. Many research projects use E2 as representative of emerging pollutant (EP) for water tertiary treatment study and photodecomposition improvement [8].

There are many studies of immobilized TiO$_2$-based composites, TiO$_2$- and iron-exchanged zeolite of ZSM5 type (TiO$_2$-FeZ), or another semiconducting material (TiO$_2$-SnS$_2$) and active solar photocatalysts. The solar-driven photocatalytic parameters as pH values, H$_2$O$_2$ concentration, and composite formulation, on the effectiveness of E2 degradation, allow the calculation of the surface modeling. The solar/TiO$_2$-FeZ/H$_2$O$_2$ process achieved E2 degradation by 78.1%; it was higher in comparison with the reference process of TiO$_2$ P25 with 41.3% of remotions and

the solar/TiO_2-SnS_2 and solar/TiO_2-SnS_2/H_2O_2 processes with 51.0 and 34.4%, respectively. The E2 degradation by solar/TiO^{2-}FeZ/H_2O_2 enhances in the presence of NOM, as real water constituents. On the other hand, the nitrates and carbonates presence show an inhibitory effect.

There are many studies using visible photodecomposition of the hormones such as estrone (E1), 17β-estradiol (E2), estriol (E3), and 17β-ethinylestradiol (EE2) with the concentration in the interval of 0.004–5.00 mg L^{-1} using TiO_2 in porous sheets, microcrystalline glass plates, P25 suspension, UVC/H_2O_2, solar Fe II, and ozone 30 mg L^{-1}. The process usually includes UV and visible light from 280 to 400 nm and full spectrum from 200 nm to 30 μm, and LED lamp with the lines at 382 nm, 254 nm, and 254 high intensity. The kinetics of such process was from 550×10^{-3} min^{-1} (pH 5) to 3.4 min^{-1} (20°C) with and without H_2O_2 with solar light 86% in 60 min and 63.9% in 12 min. The hormones enter in the water environment mainly from the sewage discharge and the effluent of sewage treatment plants. The EE2 is the main composition of the oral contraceptives, and E1, E2, and E3 occur naturally. The estrogenicity order is EE2 > E2 > > E1>>>> > E3. Most of the hormones show photodegradation over immobilized TiO_2 sheets under UV-LED irradiation or solar radiation following the first-order kinetics, faster at pH 4.

The most efficient hormone decomposition is the combination of the photo-decomposition and ozonation using TiO_2-coated glass with LED irradiation on λ = 382 nm. The application of such a dynamic process removes about 22 chemical priority substances and contaminants of emerging concern, including the resistant bacteria and genes after discharge in surface water resources. There was no compound with estrogen effect formed after the reaction; the process improves the removal efficiency of microbial loads.

The improvement of the EE2 degradation, clofibric acid, nonylphenol, and carbamazepine was slightly by the use of ultrasound combined with ozonation and photodecomposition. The removal percentage increases with pH, but at higher pH also showed an adverse decomposition effect.

The test in vitro can detect estrogen receptor agonists and antagonists. However, the estrogen-disrupting compounds do not only act on the estrogen receptor but also inhibit enzymatic catalysis reactions and the transport of hormones in the blood or the hormone production. Only in vivo analysis with a full spectrum of possible mechanisms can be identified in a whole organism.

The photocatalytic degradation of 17α-ethynylestradiol (EE2) allows the identification of 12 intermediates. The decomposition efficiency of EE2 decreased at pH 3 and in the presence of methanol at pH 7. The study proposes three degradation pathways: (1) the transformation of the phenolic ring, (2) the photocatalytic degradation of the aliphatic carbon linked to the aromatic ring at pH 7, and (3) the isomerization of EE2 in the presence of methanol at pH 7. The EE2 photocatalytic degradation is pH-dependent and at pH of 3, 7, and 10 without methanol addition were 63, 72, and 99%, respectively. The pH increase facilitated the formation of hydroxyl or hydroperoxyl disubstituted intermediates. In aqueous solutions, aliphatic carboxylic acid decarboxylation is preferable to the corresponding reduced hydrocarbons; some published results indicate the favored pathway for dicarboxylic acid mineralization is the decarboxylation resulting from the photo-Kolbe reaction [Eq. (3)]. The responsible for the formation of intermediary compounds is the attack of the ˙OH and ˙OOH radicals:

$$RCOO^- + h^+ \rightarrow R^\cdot + CO_2 \ (photo - Kolbe) \qquad (3)$$

First was the oxidation of the EE2 and then the reduction to EEO in the presence of h$^+$ and electron, formed by the methanol radical as described in [Eqs. (4)

and (5)]. Under acidic conditions, there is the inhibition of the radical methanol production. Alternatively, under alkaline condition, very little free h^+ existed in the solution, and the formation of EEO only occurred under neutral pH conditions:

$$h^+ + CH_3OH \rightarrow CH_3O^{\cdot} + H^+ \tag{4}$$

$$CH_3O^{\cdot} \rightarrow H_2CO + H^+ + e^- \tag{5}$$
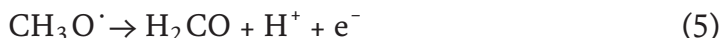
The photodecomposition of methanol acts as an $^{\cdot}OH$ scavenger and retards the photocatalytic degradation of EE2 reducing for only 8, 11, and 15% at pH of 3, 7, and 10, respectively, with methanol presence. Published researches indicate just the addition of a small amount of methanol or toluene inhibited the photocatalytic oxidation.

The formation of the intermediate products was in low mineralization rate and low removal efficiencies, resulting in total organic carbon less than 20% with the occurrence only of the phenolic ring transformation during the reaction.

7. Solar treatment for acetaminophen and antipyrine contamination

The acetaminophen (ACE) is one of the most widely used analgesics and antipyretic drugs and is one of the top pharmaceuticals prescribed in the USA or England, being China the second ACE manufacturer. It is present in surface water bodies as a result of 60–70% of human excretion via urine after medicine consumption [9]. The ACE water detection in the USA and Europe on sewage treatment plant and their effluents was in concentrations of 10 to 65 μg L^{-1}. In population, such water pollution may lead to hepatic necrosis caused by its transformation to N-acetyl-benzoquinone imine upon oxidation, which can hydrolyze to 1,4-benzoquinone; both by-products are toxic of significant concern.

The antipyrine (ANT) detection is common in sewage and polluted surface water. Such anti-inflammatory compound is a nonsteroidal and antipyretic drug which enters in the aquatic environment after use. Environmental accumulation causes adverse human health effects and affects aquatic life. The concentrations of emerging contaminants in the influent and effluent from wastewater treatment plants showed the concentration of ANT was relatively low (about 0.04 mg L^{-1}), and about 68.5% escaped from conventional activated sludge wastewater treatments, allowing to reach surface water resources.

TiO$_2$ is still the widest semiconductor used for ACE and ANT photodegradation due to its low cost, nontoxicity, and chemical stability. Nevertheless, the difficulty of TiO$_2$ recovery after the reaction and the relatively limited adsorption capacity with low surface area and porosity are some of the technological disadvantages.

There is no acetaminophen degradation versus time under solar irradiation in the absence of photocatalyst after 6 h; the removal using different photocatalysts without light irradiation also can be considered negligible (lower than 6%). The sensitization of TiO$_2$ by the carbon material titanium nanotubes and C-Ti showed a significantly higher activity than the non-modified Ti. However, the acetaminophen removal remained below 70% after 4 h of illumination. The lack of anatase crystal structure is responsible for the small photoactivity; the amorphous titanium is not active. The air calcination at above 300°C had a beneficial effect on C-Ti catalyst; the calcined samples at 400 and 500°C allowed the total acetaminophen conversion in only 1 h. The crystallization of TiO2 explains the effect into anatase (with a bandgap energy of 3.12 eV), which is the most active titanium phase for photocatalytic

applications; at the lowest calcination temperature tested (300°C), there is no significant crystallization of anatase.

Published results indicated the pseudo-first-order rates were 0.13, 0.19, and 0.38 h^{-1} for complete photodecomposition of antipyrine, acetaminophen, and ibuprofen, respectively. Regarding with the properties of the C-TiO_2 semiconductor materials, the structured defects caused by the C incorporation (as substitutional anion or interstitial cation) are the responsible for the photocatalytic activity of these materials, acting as trap centers or the photogenerated charges.

The investigation of the role of the reactive oxygen species used selected scavengers as isopropanol, the OH radical scavenger; the addition reduced the degradation rate. The OH radicals are very reactive, and the reduction by the scavenger inhibited the degradation rate, an indication of the involvement of the OH radical production in acetaminophen photodegradation. Some references mentioned the O_2^- radicals attack preferentially organic compounds with aromatic rings (as ACE aromatic ring).

8. Photodecomposition of bisphenol a (BPA)

BPA is present in polycarbonate plastics and epoxy resins such as plastic water bottles, many food containers, water pipes, medical equipment, dental sealants, thermal receipts, electronics, and toys [10, 11]. The compound is toxic for the reproductive system because it mimics the human hormone estrogen. BPA production in the world exceeds 3 million tons per year. The BPA presence in the environment results in adverse effects on organic metabolism such as reproduction, metabolic systems, organism development, neural networks, and cardiovascular irrigation. The use of BPA is mostly as a plastic monomer, the monomer for epoxy, polycarbonate plastics, and epoxy resins. About all studied environment compartments have in some degree any content of BPA including air, water, and soil [9]. Published works indicate a connection between the BPA exposition and high levels of anxiety, depression, hyperactivity, and inattention. The BPA detection in organic body demonstrated its presence in blood, urine, cardiovascular diseases, diabetes, and obesity, posing a risk for fetal development and reducing the basal testosterone secretion. There is also a combination of BPA presence and other similar compounds in environmental compartments, food and food containers, and also in humans' milk, urine, and placental tissue; this is evidence of the possible global exposition.
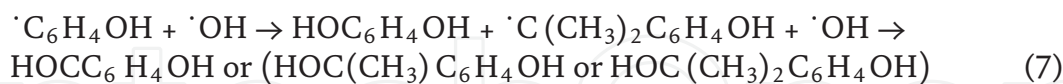
The use of spiked sodium hypochlorite removes BPA from real water samples at 50 mg L^{-1} for 10 min with a removal percentage of 99%. In spite of the formation of chlorinated by-products during the process with some toxic side effects. The advanced UV/H_2O_2 was able to remove 85% of the initial BPA at 240 min. However, a high level of the H_2O_2 is essential to execute such BPA removal process. The presence of carbonates and bicarbonates reduces the UV/H_2O_2 efficiency due to scavenging radical's formation. The ozonation is an excellent option but is extremely costly and is suspected to form intermediates which carcinogenic nature [12].

The concentration = 20 mg L^{-1}, TiO_2 dosage = 0.5 g L^{-1}, initial pH = 7.0, and temperature = 25°C followed the first-order model. The possible mechanisms for BPA photodegradation are in the following sequence:

1. Initial photooxidation, proceeded by electrophilic hydroxyl radicals ($^\cdot$OH), produced the photocleavage of electron-rich carbons in the phenyl groups of BPA or the excited BPA molecules attacked by hydroxyl radicals ($^\cdot$OH) forming phenol radicals ($^\cdot C_6H_4OH$) and isopropylphenol radicals ($^\cdot C(CH_3)_2C_6H_4OH$) [Eq. (6)].

$$HOC_6H_4C(CH_3)_2C_6H_4OH + (^{\cdot}OH) \rightarrow {^{\cdot}C_6H_4OH} + {^{\cdot}C(CH_3)_2C_6H_4OH} \quad (6)$$
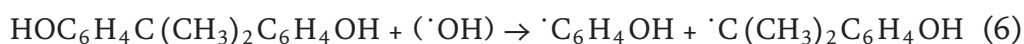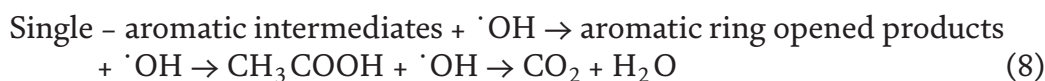
2. The hydroxyl radical ($^{\cdot}OH$) converted to p-hydroquinone (HOC_6H_4OH) and isopropylphenol radical allow the formation of the 4-hydroxyphenyl intermediates such as p-hydroxybenzaldehyde, p-hydroxyacetophenone, and 4- hydroxyphenyl-2-propanol [Eq. (7)].

$${^{\cdot}C_6H_4OH} + {^{\cdot}OH} \rightarrow HOC_6H_4OH + {^{\cdot}C(CH_3)_2C_6H_4OH} + {^{\cdot}OH} \rightarrow$$
$$HOCC_6H_4OH \text{ or } (HOC(CH_3)C_6H_4OH \text{ or } HOC(CH_3)_2C_6H_4OH) \quad (7)$$

3. The oxidation reaction of the single-aromatic intermediates through ring-opening reactions results in aliphatic acids.

The pH values decrease in aqueous media gradually, and the intermediates were entirely mineralized of forming carbon dioxide (CO_2); the oxidization of the aromatic intermediates occurs subsequently through ring-opening reactions into aliphatic acids [Eq. (8)].

$$\text{Single} - \text{aromatic intermediates} + {^{\cdot}OH} \rightarrow \text{aromatic ring opened products}$$
$$+ {^{\cdot}OH} \rightarrow CH_3COOH + {^{\cdot}OH} \rightarrow CO_2 + H_2O \quad (8)$$

The UV-A radiation ($\lambda = 365$ nm) with TiO_2 P25 result in complete removal after 180 min in first-order kinetics with Kap = 20.3 10^{-3} min^{-1}, with 5 mgL^{-1} as initial concentration and 200 mg L^{-1} as the addition of the TiO2 P25 [3]. The complete mineralization of BPA was at pH 3 after 120 min; intermediates formed at higher pH values are most stable and therefore difficult to be decomposed and mineralized [13, 14]. The TiO_2 sources as anatase, rutile, brookite, and their mixtures indicate the lower uptakes with less than 6% were over the raw TiO_2. The anatase and rutile TiO_2 mixtures obtain 94 and 80% of removal percentage, respectively, higher than the obtained for the anatase, rutile, and brookite single composition. The mixture anatase/TiO_2 brookite reached the complete mineralization, and the mixture of anatase and rutile was five-fold slower than the commercial TiO_2 P25 with 3 min of complete removal percentage. All products showed less toxicity and estrogenic activity than the initial BPA [15, 16].

The nano-TiO_2 facilitates the degradation under sunlight radiation with O_2^{-2} as dominant oxidizing species. The better degradation efficiency was at pH 2.6, and correspondent with the pseudo-first-order without nanoparticles was one or two orders small with $\lambda = 365$ nm of radiation using pristine nanotubes [10].

The higher results were with anatase particles enhanced by the presence of rutile and preferential oxidation of reaction intermediates on brookite. The toxicity removal was for TiO_2 supported on a glass fiber with UV light radiation $\lambda = 365$ nm in batch and stirrer tank.

The use of a wide range of metals as the lanthanum-doped TiO_2 was able to degrade BPA completely under acidic conditions within 2 h; the result is far better than undoped TiO_2.

The oxidants' addition enhances efficiency, as H_2O_2 and FeII. The H_2O_2 interacted with Fe-2þ ions to produce hydroxyl radicals. The Fe doped into the TiO_2 decreased the bandgap, which also enhanced the BPA photodegradation. The addition of 5 mol% of Fe in TiO_2 successfully removed 10 ppm of BPA in 2 h. The experiment with nitrogen doping on TiO_2 indicated the N-doped TiO_2 enhanced the photodegradation of BPA compared to conventional TiO_2. Likewise, the iodine-doped TiO_2, upon exposure to UV and visible irradiation, showed increased degradation efficiencies for BPA up to 93 and 100%, respectively.

The 4-chlorophenol, phenol, methylene blue, rhodamine B, and acid orange presence reduces the surface area for the volume and enhances the oxygen vacancies in TiO_2 surface matrix by N-doping and F-doping, and surface acidity is also improved by F-doping, and visible light adsorption by N-doping of nitrogen-fluorine-codoped TiO_2 photocatalyst. The use of simulated sunlight lamps promotes the generation of the active species for BPA decomposition as O_2^{-2}.

The production of TiO_2 PEG started with the mixture of titanium ethoxide and ethanol solution followed by PEG addition; the suspension aged for 24 h and calcined for 2 h at 400°C. The optimization of the TiO_2 production by sol–gel polyethylene glycol (PEG) includes the variation of the PEG molecular weight, the mass percentage, the pH, and the TiO_2 dose. The visible light BPA degradation rates for TiO_2 with PEG200 (10%), PEG600 (5%), and PEG3500 (0.5%) at pH 4 were 2.07, 3.01, and 2.90 h^{-1}, respectively. After 12 h of reaction, the total organic carbon measurements indicated a small BPA degradation with the reduction of TiO_2, with PEG200 (10%), PEG600 (5%), and PEG3500 (0.5%) of 38%, 56%, 65%, and 64%, respectively. The content of hydroxyl radicals in TiO_2, with PEG200 (10%), PEG600 (5%), and PEG3500 (0.5%), was 50.1, 88.6, 78.8, and 75.1 µM, respectively. Allowing the conclusion about the PEG addition on the TiO_2 preparation increases the photoactivity, and the optimal PEG addition percentage varied with PEG molecular weight and content.
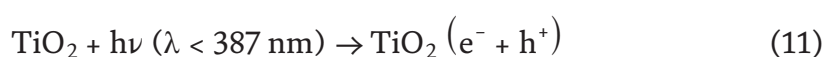
9. Antibiotic photodecomposition

The antibiotic removal and other anthropogenic compounds by adsorption are the major chemical process of deactivation, and it is important to reduce the toxic properties and to restrict their transport into water systems. The adsorbent material in combination with titanium dioxide or titania (Ti) showed better results using adsorption combined with photocatalytic activity with low cost, nontoxicity, and high stability in aqueous solution. Nevertheless, the disadvantages of TiO_2 powders are the low surface area (Degussa P25 = 35–45 $m^2\,g^{-1}$, anatase < $m^2\,g^{-1}$); the anatase bandgap of 3.20 eV uses only a small UV fraction of solar light, about 2–3%, with the high cost of the TiO_2 powder separation and recovery from treated wastewater [17, 18].

The removal of tetracycline (TC) by TiO_2 and the mesoporous binary system TiO_2-SiO_2 was tested, and it is strongly dependent on pH, with increasing pH it decreases. The electrostatic forces and H-bond formations mainly between amide, carboxylic, and phenolic groups of the antibiotic and the functional groups of TiO_2 are also important. The adsorption capacity increases in the following order TiO_2 < TiO_2-SiO_2 (high surface area). The photodegradation rate is affected by pH 7 or lower; the related mechanism is to $OH^{\cdot}$ radicals—the composed titania-silica act as an adsorbent and alternative photocatalyst for pollution control.

All processes result in high degradation efficiency of the β-lactam antibiotic (oxacillin). The $TiO2$ photocatalysis, the sonochemistry, the photo-Fenton process, and electrochemistry (with a Ti/IrO2 anode in sodium chloride solution). The processes are successful ,but three of them involve the hydroxyl radical generation and the degradation pathways, by-products' generation, and the mineralization degree. The electrochemical process performed the decomposition by chlorine production and its attack when the sonochemical and photo-Fenton systems have the production of the hydroxyl radical.

The high oxidant species with low selectivities, such as hydroxyl radicals (E = 2.8 V), are formed in advanced oxidation processes (AOPs) and the active chlorine electrogenerated through dimensionally stable anodes (DSA). The irradiation of an aqueous suspension of TiO_2-semiconductor with UV light produces hydroxyl radical.

The TiO_2 photocatalysis combines the holes' generation with the attack of the hydroxyl radicals. The by-product analysis indicated the four oxidation processes exhibited the oxidation of the thioether radical followed by the amide breakdown and finally the β-lactam opening ring. However, the antibiotic decarboxylation was only a result of the TiO_2 photocatalysis, explained by the holes' production with direct oxacillin oxidation [Eqs. (9)–(15)]. The electrochemical process promotes the oxacillin isomerization pathway, while the photo-Fenton and TiO_2 photocatalysis treatments showed hydroxylation at the aromatic ring. The different degradation routes generated different mineralization extent and efficiency [19].

$$P + {}^{\cdot}OH \rightarrow Pox \tag{9}$$

$$HClO, ClO^-, Cl_2 + P \rightarrow Pox \tag{10}$$

$$TiO_2 + h\nu \ (\lambda < 387 \ nm) \rightarrow TiO_2 \left(e^- + h^+\right) \tag{11}$$

$$h^+ + H_2O \rightarrow H^+ + {}^{\cdot}OH \tag{12}$$

$$h^+ + OH^- \rightarrow {}^{\cdot}OH \tag{13}$$

$$h^+ + P \rightarrow P_{ox} \tag{14}$$

$$e^- + O_2 \rightarrow {}^{\cdot}O^-{}_2 \rightarrow \rightarrow {}^{\cdot}OH, {}^{\cdot}OOH, H_2O_2 \tag{15}$$

The total organic carbon measurements in TiO_2 photocatalysis and the photo-Fenton system were 90 and 35%, respectively, and with just the sonochemical and electrochemical treatments, the pollutant was not mineralized.

The presence of the ultrasonic waves in aqueous solutions is another way to form hydroxyl radicals [Eqs. (16)–(19)]. Singular conditions of temperature (5000 K) and pressure (1000 atm) induce the formation of ultrasonic microbubbles which violently collapse in water, and the dissolved oxygen is dissociated to produce hydroxyl radicals.

$$H_2O +))) \rightarrow {}^{\cdot}H + {}^{\cdot}OH \tag{16}$$

$$O_2 +))) \rightarrow 2{}^{\cdot}O \tag{17}$$

$$H_2O + {}^{\cdot}O \rightarrow 2{}^{\cdot}OH \tag{18}$$

$$O_2 + {}^{\cdot}H \rightarrow {}^{\cdot}O + {}^{\cdot}OH \tag{19}$$

The reaction of Fe (II) with hydrogen peroxide produces radicals. The reduction of Fe (III) in aqueous media results in Fe (II) by the action of UV–Vis light and extra hydroxyl radicals in a photo-Fenton process.

The electrochemical oxidation which soluble chloride results in chloride anions on the Ti/IrO_2 anode [Eq. (20)] which the generation of hypochlorous and hydrochloric acids [Eq. (21)]. The dissociation of the hypochlorous acid forms

hypochlorite [Eq. (22)]. Chlorine, hypochlorous acid, and hypochlorite are active species, and they are very dependent on the pH values. The predominant species at pH lower than 3 is Cl_2 (E = 1.36 V), in the range of pH 3 to 8 is $HClO^-$ (E = 1.49 V), and at pH higher than 8 is OCl^- (E = 0.89 V).

$$2Cl^- \rightarrow Cl_2 + 2e^- \qquad (20)$$

$$Cl_2 + H_2O \rightarrow HClO + HCl \qquad (21)$$

$$HClO^- + H_2O \rightarrow ClO^- + H_3O^+ \qquad (22)$$

The knowledge of the oxidation routes in water treatment can optimize the process and establish a pollutant degradation mechanism and pathways: the experimental parameters and the matrix influence on oxacillin (OXA) on electrochemical oxidation and TiO_2 photocatalysis. Here is no report about photo-Fenton and sonochemical processes' removal of oxacillin from polluted water.

The sonochemical process degraded the antibiotic and generates solutions without OXA entirely; the antimicrobial activity showed an excellent performance and adjustment to exponential kinetic-type decay, and the degradation rates were 1.4 μM min^{-1} for OXA, 1.3 μM min^{-1} for OXA with mannitol, and 1.4 μM min^{-1} for OXA with calcium carbonate. The possible OXA sonic degradation mechanism was proposed based on the evolution of the by-products and their chemical structure [Eqs. (16) and (17)] [20].

The ultrasound application over 120 min removed OXA compounds and eliminated its antimicrobial activity. However, the mineralization was not reached even after (360 min). The mineralization of the oxacillin under previous water sonication reduce the microbial activity even with non-adapted microorganisms from a municipal wastewater treatment plant. The results showed the sonochemical transformation of the initial pollutant into biotreatable substances even using the typical aerobic biological system.

The iron ions present in the matrix affect the antibiotic (OXA) decomposition, with improvement in degradation, and the inhibition was by the addition of pharmaceutical excipients of a commercial formulation or by inorganic ions of natural mineral water. The best performances were achieved at natural pH 6.0 using 2.0 g L^{-1} of TiO_2 with 150 W of light intensity. The OXA photodegradation process showed a Langmuir-Hinshelwood kinetic model. The achievement of the total antibiotic removal was after 120 min, with 100% of mineralization. Finally, the identification of five by-products elucidates the degradation routes with a proposition of an antibiotic degradation (**Figure** 2).

The addition of 2-propanol as a scavenger, 25 times higher than the antibiotic, produces a slight reduction (about 3%) in the antibiotic removal rate, and the concentration of 645 times higher than the OXA causes 30% of inhibition. The result indicates the hydroxyl radicals present at the solution may contribute to the degradation of the antibiotic molecules. The essays in the presence of KI concentration 25 times higher than the OXA concentration showed 75% of inhibition. The use of equimolar KI concentration resulted in a 13% reduction. The indication of the degradation rate is in association with adsorption reduction of the catalyst surface. Consequently, the degradation of OXA by heterogeneous photocatalysis seems to occur mostly at the catalyst surface and via two routes: by the radical attack and photo-Kolbe mechanism.

The UV irradiation of antibiotic molecules generates excited states and the detection of such reactive species by an indication of their ability to oxidize luminal reagent. Such compound uses the electronically excited aminophthalate, which
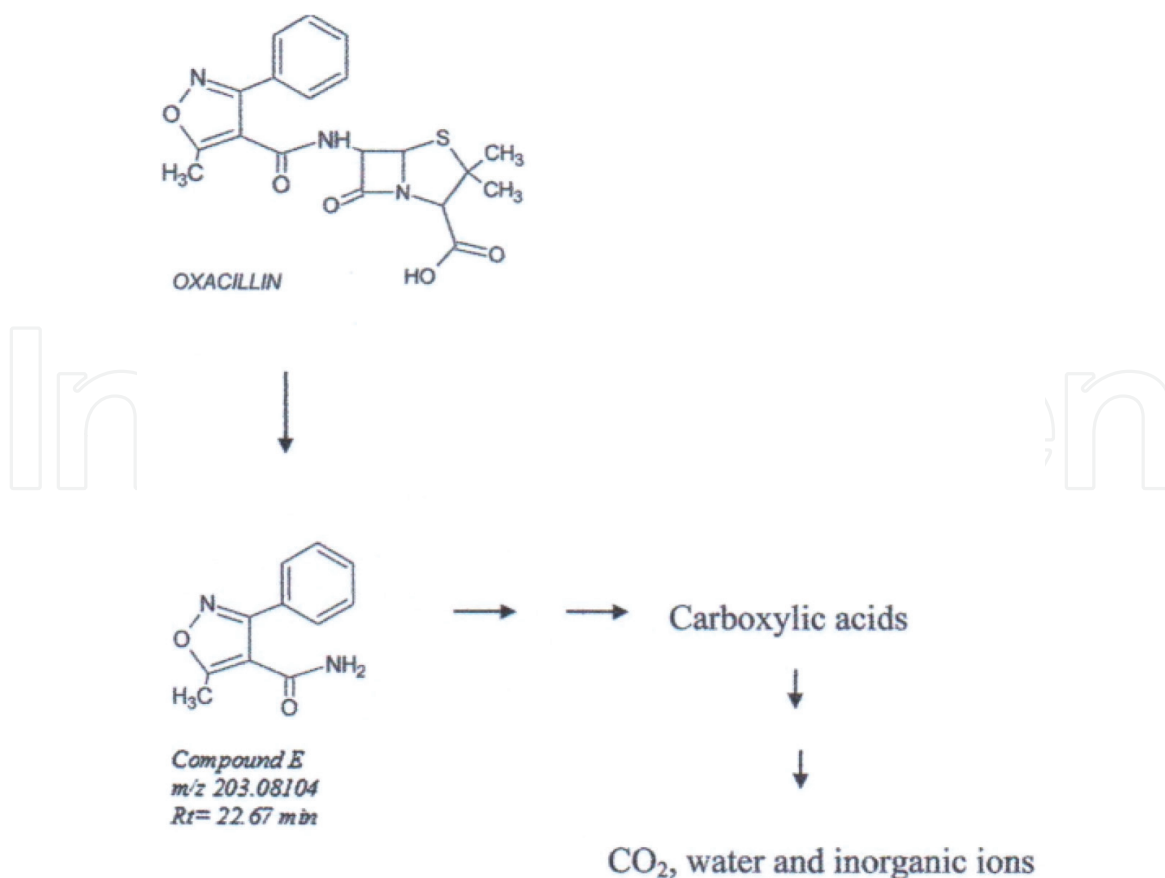
Figure 2.
Oxacillin photodegradation pathway.

decays to the ground state releasing electromagnetic radiation in the visible zone of the spectrum—the application of the method to penicillin G, nafcillin, azlocillin, and neomycin dissolved in water. The intensity of the luminal chemiluminescence emission (CL) was proportional to the radical concentration and dependent on the molecular structure of the drugs. Under the optimized conditions, the penicillin and azlocillin were the most susceptible to photodegradation, while neomycin sulfate was less affected by the UV light. The addition of a hydroalcoholic extract of rose petals to antibiotic solutions reduced the CL intensity, indicating the alcohol act as a scavenger of free radicals of the irradiated drugs.

10. Synergistic effect

In the application of the solar photodecomposition in the dye mixture of RH and MB, the result is similar with a single dye, and the adsorption balance remains unchanged with no interaction between RH and MB and their by-products. Nevertheless, the addition of MO in the mixture accelerated the photodecomposition significantly. The decomposition of RH/MO and the MB/MO reduced the decomposition time in 13 and 10 min, respectively [21]. Such an effect is positively dependent on the MO concentration; the application of Eq. (23) to the Langmuir-Hinshelwood model

$$-\ln(C/C_o) = k'Kt = kt \qquad (23)$$

where C_o and C are the initial and t measured concentrations, t is the reaction time, and k are the first-order-kinetic reaction constant, calculated using $\log(C/C_o)$ vs. t.

The kinetics k rate indicates higher values for binary systems with MO component. When the MO concentration reaches a constant value, the reaction depends on the photocatalyst mass. The preparation of ternary mixtures with RH or MB and different azo species as orange G (OG), methyl red (MR), and Eriochrome Black T (EBT) clarifies the reaction mechanism dependency. The synergistic effect after azo compound addition is confirmed, and the time decreases about 23 and 13 min for RH and MB, respectively.

The photodecomposition acceleration effect is positively proportional to the azo dye concentration and no longer changes after reaching a specific equilibrium value. The comparison with the k values indicates higher rates for EBT > OG > MO > MR; the sequence is in agreement with the polarity of the four azo dye compounds. The azo compounds in the experiments were acid orange 7 (AO7), Congo red (CR), and amido black 10B (AB10B). The results were the same obtained for the other azo compounds confirming the synergistic oxidation effect.

The possible decomposition mechanism includes the highest occupied molecular orbital (HOMO) and the lowest unoccupied molecular orbital (LUMO) as a type of molecular frontier orbitals. Roughly, the HOMO level is for organic semiconductors, the equivalent of the valence band for the inorganic semiconductors, and the LUMO is the equivalent of the semiconductors' conduction band. The energy difference between them is called a HOMO-LUMO gap. The energy gap between the two frontier orbitals can be used to predict the strength and stability of the transition metal complexes and also their colors in solution.

The simulated changes of the azo molecule methylene orange (MO) in molecular energy structure in the photocatalyst Ag_2O surface indicate the LUMO composed by the atomic orbital contributions of benzene, nitrogen, and the nitrogen double bond, and the HOMO is a result of the paired electron orbits of negatively charged oxygen atoms in the sulfonic group.

After the MO adsorption in Ag_2O surface, the electrons on the surface of the Ag_2O can transfer to the molecules' LUMO and participate in feedback coordination at the bond. The C—N bond links the benzene ring to the azo group, and it becomes longer on adsorption. Such coordination effects weaken the π bonding conjugated over the whole molecular skeleton and start to be attacked by photogenerated electrons or radicals, with the presence of active fragmented intermediates. The resultant intermediates caused subsequent acceleration of azo bond cleavage also for non-azo organic cleavages due to their oxidative activity.

The infrared results of the MO adsorbed in Ag_2O indicate a shift for N=N bond from 1392 to 1396 cm^{-1}, for $-SO3^-$ was observed from 1314 and 1121 cm^{-1} to 1320 and 1120 cm^{-1}, and for C—N bonds from 817 and 749 cm^{-1} to 819 and 751 cm^{-1}. Another shift for Ag_2O was from 650 to 705 cm^{-1}. They are the confirmation of the sulfonic group acting as an electron donor and Ag_2O as an electron acceptor, weakening the conjugated π bonding and activating the N=N and C—N bonds confirming the adsorption of MO by Ag_2O. The MO peaks disappear including the sulfonic group and the azo bond after 2 min of irradiation, suggesting to be the first degraded group. The suspension started to be colorless, and the peaks assigned to be C=C bond start to appear after 5 min of exposition, an indication of the benzene rings broken. There is no observation of MO chemical structure after 10 min of light irradiation; it is an indication of the complete dye decomposition. The azo bond or C—N bond connected with the benzene rings broken first and produces active intermediates which accelerate the degradation of non-azo organics followed by the benzene ring broken.

Generally, the C—N bond linked to the benzene ring and the azo group of the MO is the first target for the free radicals produced by the photocatalyst. The possible intermediates are aminobenzenesulfonates, aromatic amines, phenolic

compounds, and organic acids. The final products, also called mineralization, are N_2, CO_2, H_2O, SO_4^-, NH_4^-, and NO_3^-.

The presence of photodecomposition intermediates to the photodegradation process of RH and Ag_2O resulted in faster decomposition. The phenol addition reduces the decomposition time to 8 min, the sulfanilic acid in 10 min, and the benzoquinone in 30 min. However, the addition of acetic acid and hydroquinone slows the RH photodegradation. Finally, the MO molecule can be decomposed into holes or radicals generated over Ag_2O and break the C—N bonds releasing the benzene containing the intermediates such as benzene sulfonate and N-N dimethylaniline. The next intermediate products were hydroxybenzenesulfonate activated by excited Ag_2O and diffused in solution accelerating the degradation of organic compounds in the Ag_2O surface.

The description of the acceleration of the photodegradation process with azo dyes' presence in a mixed dye solution is a synergy between the azo structure and Ag_2O with the generation of aniline, sulfanilic acid, and phenol compounds which also accelerates the degradation of the non-azo compounds. The synergetic effect is beneficial for the Ag_2O photodecomposition applicability to treat the ordinary real wastewater with a complex dye mixture.

11. Conclusion

Environmental sustainability demands the advance in water treatment and the use of lighting natural resources. Brazil has one of the most stable and intense solar irradiation in the word. It has to be used not only for energy generation purposes but also and mostly for water treatment, water quality polishment, and furthermore water disinfection. The chapter performs a comparison of different green technologies for water treatment as natural solar irradiation. The photocatalytic hydroxide radicals are the photodecomposition potent oxidants and react fast and unselectively with surrounding chemical species via radical addition, hydrogen abstraction, or e^- transfer mechanisms. The transformation by-products of pharmaceuticals and EDC compounds (TBPs) with higher photodecomposition effectiveness ends up in complete mineralization with the production of CO_2, H_2O, and inorganic salts. The heterogeneous photocatalysis shows a strong dependence of the operating temperature, and the kinetics is usually dependent on the first step of the adsorption and the equilibrium modeled by Langmuir isotherms and Langmuir-Hinshelwood model. The first pseudo-order usually appears at the beginning of the reaction, just in the initial steps, and as the reaction proceeds, the intermediates' production could interfere with the radiation incidence. There is a competition of the adsorption sites of the catalyzer surface between the pollutant and others adsorbed species; the pollutants start concentration is a limiting reactant step with mass transfer limitations in lower concentrations. The semiconductor TiO_2 photocatalytic process has shown great potential as a low cost, environment-friendly treatment technology in degrading a wide range of pollutants with the formation of reactive oxygen species upon excitation of a semiconductor particle with light energy greater than the respective bandgap energy of the photocatalyst. The photocatalyst TiO_2 has superior characteristics over others with wide bandgap energy which requires the UV light which is 3–5% of natural solar light. The application of a variety of strategies improved the photocatalytic efficiencies from photocatalysts as dispersed solids to second-generation photocatalysts (chemically doped and physically modified dispersed solids) achieving better spectral sensitivity and photoactivity. Many studies indicate the scavengers' presence reduces the photodecomposition effect in water suspension. The ions HCO_3^-/CO_3^{2-}, SO_4^{2-}, Cl^- and NO_3^- showed inhibitory effects

toward the hydroxyl radicals generated by AOPs; the natural organic matter (NOM) presence showed a synergistic effect increasing the E2 degradation, such degradation produces other radicals. The application of the visible light photodecomposition in a dye mixture of methylene blue (MB), methyl orange (MO), and rhodamine (RH) indicates the MO as the more stable azo compound than the other organic pollutants due to the aromatic groups attached at the end of the azo bond. Despite this fact when the light-driven photodecomposition uses the Ag_2O as a catalyzer, it was the fastest and easiest decomposed compound. Published results indicate the visible light photodecomposition with Ag_2O with the elimination of 90.2% of MO, 96.5% of RH, and 99.5% of MB using 4, 50, and 20 min, respectively. The photodecomposition acceleration synergistic effect is positively proportional to the azo dye concentration and no longer changes after reaching a specific equilibrium value. The comparison with the k values indicates higher rates for EBT > OG > MO > MR; the sequence is in agreement with the polarity of the four azo dye compounds. The azo compounds in the experiments were acid orange 7 (AO7), Congo red (CR), and amido black 10B (AB10B). The results were the same obtained for the other azo compounds confirming the synergistic oxidation effect. The possible decomposition mechanism includes the highest occupied molecular orbital (HOMO) and the lowest unoccupied molecular orbital (LUMO) as a type of molecular frontier orbitals. The description of the acceleration of the photodegradation process with azo dyes' presence in a mixed dye solution is a synergy between the azo structure and Ag_2O with the generation of aniline, sulfanilic acid, and phenol compounds which also accelerates the degradation of the non-azo compounds. The synergetic effect is beneficial for the Ag_2O photodecomposition applicability to treat the ordinary real wastewater with a complex dye mixture.

Acknowledgements

Author details

Nilce Ortiz
Institute for Nuclear and Energy Research–IPEN, São Paulo, Brazil

*Address all correspondence to: nortizbr@gmail.com

IntechOpen

References

[1] Foteinis S, Borthwick AGL, Frontistis Z, Mantzavinos D. Environmental sustainability for light-driven processes for wastewater treatment applications. Journal of Cleaner Production. 2018;**82**:8-15. DOI: 10.1016/j.clepro.2018.02.038

[2] Kovacic M, Kopcic N, Kusic H, Bozic AL. Solar driven degradation of 17β estradiol using composite photocatalytic materials and artificial irradiation source: Influence of process and water matrix parameters. Journal of Photochemistry and Photobiology A: Chemistry. 2018;**361**:48-61. DOI: 10.1016/j.jphotochem.2018.05.015

[3] Quesada-Carera R, Mills A, Rourke CO. Action spectra of P25 TiO$_2$ and visible light adsorbing, carbon-modified titania in the photocatalytic degradation of stearic acid. Applied Catalysis B: Environmental. 2014;**150-151**:338-344. DOI: 10.1016/j.apcatb.2013.12.008

[4] Kamimura S, Miyazaki T, Zhang M, Li Y, Tsubota T, Ohno T. Au@Ag@Au double shell nanoparticles loaded on rutile TiO$_2$ for photocatalytic decomposition of 2-propanol under visible light irradiation. Applied Catalysis B: Environmental. 2016;**180**:255-262. DOI: 10.1016/j.apcatb.2017.04.028

[5] Haroune L, Salaun M, Menard A, Legault CY, Bellenger J. Photocatalytic degradation of carbamazepine and three derivatives using TiO$_2$ and ZnO; effect of pH, ionic strength, and natural organic matter. Science of the Total Environment. 2014;**475**:16-22. DOI: 10.1016/j.scitotenv2013.12.104

[6] Gao X, Peng W, Tang G, Guo Q, Luo Y. Highly efficient and visible—Light driven BiOCl for photocatalytic degradation of carbamazepine. Journal of Alloys and Compounds. 2018;**757**:455-465. DOI: 10.1016/j.jallcom.2018.05.081

[7] Canle M, Pérez MIF, Santaballa JA. Photocatalyzed degradation/abatement of endocrine disruptors. Current Opinion in Green and Sustainable Chemistry. 2017;**6**:101-138. DOI: 10.1016/j.cogsc.2017.06.008

[8] Gomes-Aviles A, Penas-Garzon M, Bedia J, Rodriguez JJ, Belver C. C-modified TiO$_2$ using lignin as carbon precursor for the solar photocatalytic degradation of acetaminophen. Chemical Engineering Journal. 2018;**358**:1574-1582. DOI: 10.1016/j.cej.2018.10.154

[9] Tobajas M, Belver C, Rodriguez JJ. Degradation of emerging pollutants in water under solar radiation using novel TiO$_2$-ZnO/clay nanoarchitectures. Chemical Engineering Journal. 2017;**309**:596-606. DOI: 10.1016/j.cej.2016.10.002

[10] Reddy PVL, Kim K, Kavitha B, Kumar V, Raza N, Kalagara S. Photocatalytic degradation of bisphenol A in aqueous media: A review. Journal of Environmental Management. 2018;**213**:189-205. DOI: 10.1016/j.envman.2018.02.059

[11] Kuo C, Wu C, Lin H. Photocatalytic degradation of bisphenol A in a visible light/TiO$_2$ system. Desalination. 2010;**256**:37-42. DOI: 10.1016/j.desal.2010.02.020

[12] Tsai W, Lee M, Su T, Chang Y. Photodegradation of bisphenol A in a batch TiO$_2$ suspension reactor. Journal of Hazardous Materials. 2009;**168**: 269-275. DOI: 10.1016/j.hazmat.2009.02.034

[13] Bechambi O, Jlaiel L, Najjar W, Sayadi S. Photocatalytic degradation of bisphenol A in the presence of Ce-ZnO: Evolution of kinetics, toxicity and photodegradation mechanism. Materials Chemistry and Physics.

2016;**173**:95-105. DOI: 10.1016/j.
matchemphys.2016.01.044

[14] Uyguner-Demirel CS, Birben
NC, Bekbolet M. Elucidation of
background organic matter matrix
effect on the photocatalytic treatment
of contaminants sing TiO_2: A review.
Catalysis Today. 2017;**284**:202-214. DOI:
10.1016/j.cattod.2016.12.030

[15] Mboula VM, Héquet V, Andrés Y,
Gru Y, Collin R, Dona-Rodriguez JM,
et al. Photocatalytic degradation of
estradiol under simulated solar light
and assessment of estrogenic activity.
Applied Catalysis B: Environmental.
2015;**162**:437-444. DOI: 10.1016/j.
apcatb.2014.05.026

[16] Sun W, Li S, Mai J, Ni J. Initial
photocatalytic degradation
intermediates/pathways of 17 α
ethynylestradiol: Effect of pH
and methanol. Chemosphere.
2010;**81**:92-99. DOI: 10.1016/j.
chemosphere.2010.06.051

[17] Serna-Galvis EA, Silva-Agredo J,
Giraldo AL, Florez OA, Torres-Palma
RA. Comparison of route, mechanism,
and extent of treatment for the
degradation of a β lactam antibiotic by
TiO_2 photocatalysis, sonochemistry,
electrochemistry, and the photo-Fenton
system. Chemical Engineering Journal.
2016;**284**:953-962. DOI: 10.1016/j.
cej.2015.08.154

[18] Serna-Galvis EA, Silva-Agredo J,
Giraldo-Aguirre AL, Florez-Acosta
OA, Torres-Palma RA. High-
frequency ultrasound as an elective
advanced oxidation process to remove
penicillin antibiotics and eliminate its
antimicrobial activity from the water.
Ultrasonics Sonochemistry. 2016;**31**:
276-283. DOI: 10.1016/.ultsonch.2016.
01.007

[19] Giraldo-Aguirre AL, Erazo-Erazo
E, Florez-Acosta OA, Serna-Galvis EA,
Torres-Palma R. ATiO_2 photocatalysis

applied to the degradation and
antimicrobial activity removal
of oxacillin: Evaluation of matrix
components, experimental parameters,
degradation pathways and identification
of organics by-products. Journal of
Photochemistry and Photobiology
A: Chemistry. 2015;**311**:95-103. DOI:
10.10167/j.photochem.2015.06.021

[20] Brigante M, Schulz PC. Remotion
of the antibiotic tetracycline by titania
and titania-silica composed materials.
Journal of Hazardous Materials.
2011;**192**:197-1608. DOI: 10.1016/j.
jhazmat.2011.06.082

[21] Bi N, Zheng H, Zhu Y, Jiang
W, Liang B. Visible-light-driven
photocatalytic degradation of non-azo
dyes over Ag_2O and its acceleration
by the addition of azo dye. Journal of
Environmental Chemical Engineering.
2018;**6**:3150-3160. DOI: 10.1016/j.
jece.2018.04.047